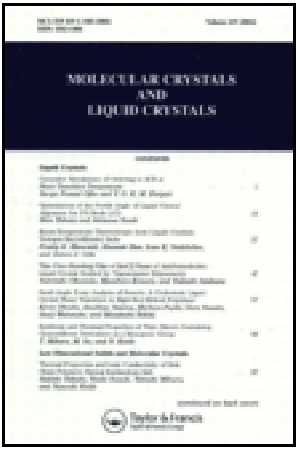

Molecular Crystals and Liquid Crystals Science and Technology. Section A. Molecular Crystals and Liquid Crystals
Publication details, including instructions for authors and subscription information:
http://www.tandfonline.com/loi/gmcl19

Liquid Crystalline Composite Based on a Clay Mineral

M. Kawasumi [a] , A. Usuki [a] , A. Okada [a] & T. Kurauchi [a]

[a] Toyoto Central Research and Development Laboratories Inc., Nagakute-cho, Aichi, 480-11, Japan

To cite this article: M. Kawasumi , A. Usuki , A. Okada & T. Kurauchi (1996): Liquid Crystalline Composite Based on a Clay Mineral, Molecular Crystals and Liquid Crystals Science and Technology. Section A. Molecular Crystals and Liquid Crystals, 281:1, 91-103

To link to this article: http://dx.doi.org/10.1080/10587259608042236

Mol. Cryst. Liq. Cryst., 1996, Vol. 281, pp. 91–103
Reprints available directly from the publisher
Photocopying permitted by license only

Liquid Crystalline Composite Based on a Clay Mineral

M. KAWASUMI*, A. USUKI, A. OKADA and T. KURAUCHI

Toyoto Central Research and Development Laboratories Inc., Nagakute-cho, Aichi, 480-11, Japan

(Received December 8, 1994; in final form December 8, 1994)

Novel liquid crystalline composites (LCC) based on a nematic liquid crystal and fine plate-like caly minerals have been prepared by mixing the two components. The observation of the LCCs by a polarized optical microscope revealed that the plate like particles of the clay mineral were dispersed homogeneously and their sizes were about several micrometers or less. In a nematic phase, the LCCs exhibit a very fine multidomain. structure which is the cause of a light scattering effect of the LCC cells. When an electric field was applied to the cell, it became transparent from milky white. Even after the electric field was switched off, the transparent state was maintained, thus exhibiting memory effect. After 3 months, no change in the transparency of the memory state was observed. Also, the thermo-optic effect of the LCC cells was discussed.

Keywords: Liquid crystalline composite, montmorillonite clay, electrooptic memory effect, light scattering effect.

INTRODUCTION

The optical memory effects of liquid crystalline materials have been reported in various electro-optical systems based on light scattering. The existence of a memory effect[1–6] in cholesterics has been evidenced by Heilmeier and Goldmacher[1]; when subjected to a dc or low frequency electric field, a cholesteric structure with smal pitch can be switched from transparent to milky white. When the field is turned off, the scattering state is still observed several hours. Similar memory effect has been found in the mixture of polymeric liquid crystals with low molecular weight liquid crystals in a smectic phase by Kajiyama *et al.*.[7–9] The mixture can be switched between a transparent state (high frequency electric field) and light scattering state (dc or low frequency electric field). Both states are stable even after the electric field is switched off. Also, the polymer dispersed liquid crystals with polyball type morphology has been reported to exhibit a memory effect.[10,11] Initially, it exhibits a light scattering state which can be switched to a transparent state by an electric field. After the field is off, the transparent state is maintained.

In this paper, we present a novel approach to add a memory effect to liquid crystals by applying a hybrid technique with inorganic particles. The novel liquid crystalline composites (LCC) based on a nematic liquid crystal and fine plate-like clay minerals, i.e. montmorillonite intercalated with a mesogenic ammonium ion have displayed a unique light scattering electro-optic and thermo-optic effect with memory effect, which can be controlled by external fields such as electric field, thermal change and shearing.

EXPERIMENTAL

Materials

4-Pentyl-4′-cyanobiphenyl (5CB) (from BDH), 4-cyano-4′-hydroxybiphenyl (95%), dimethylsulfoxide (DMSO) (both from Tokyo Chemical Ind. Co.), N-(4-bromobutyl) phthalimide (98%, from Aldrich), hydrazine monohydrate, acetone, anhydrous potassium carbonate, tetrahydrofuran (THF), hydrochloric acid, absolute ethanol, N,N-dimethylacetamide (DMAc) (all from Wako Pure Chemical Ind. Co), and pure sodium montmorillonite (cation exchange capacity: 119 meq./100 g, from Kunimine Ind. Co.) were used as received.

The preparation of montmorillonite intercalated with 4-(4′-cyanobiphenyl-4-oxy) butyl ammonium (6)

The synthetic scheme of the montmorillonite intercalated with 4-(4′-cyanobiphenyl-4-oxy) butyl ammonium (6) is shown in Scheme 1. The detailed procedures are explained below.

Sythesis of 4-(4-(N-phthalimide) butoxy-4′-cyanobiphenyl (3)

To a 250 ml three necked flask equipped with nitrogen in-outlets, reflux condenser, and magnetic stirrer, were added 10.5 g (54 mmol) of 4-cyano-4′-hydroxybiphenyl (2), 18.8 g (136 mmol) of anhydrous potassium carbonate, and acetone-DMSO mixed solvent (125ml – 12ml). The mixure was heated to the reflux temperature under stirring. After about 2 hr, 15.2 g (54 mmol) of N-(4-bromobutyl) phthalimide (1) was added and it was stirred for 17 hr. The reaction mixture was poured into 500 ml of water to yield white precipitates. The precipitates were collected on a glass filter and dried in vacuo. The product was purified by silicagel column chromatography (solvent: chloroform) followed by the crystallization from a mixed solvent (ethanol: chloroform = 3:2) to yield needlelike crystals (14.1 g) (yield, 66.0%). Melting point, 148°C.

Synthesis of 4-(4-aminobutoxy)-4′-cyanobiphenyl (4)

To a 250 ml three necked flask equipped with nitrogen in-outlets, reflux condenser, and magnetic stirrer, were added 13.9 g (35 mmol) of 4-(4-(N-phthalimide) botoxy)-4′-cyanobiphenyl (3) and 120 ml of THF. The mixture was heated to 50°C. Hydrazine monohydrate (11.1 g, 221 mmol) and 50 ml of ethanol were added and the mixture was stirred for 4 hr under reflux. Hydrochloric acid (40 ml) was added slowly. The reaction mixture was extracted with 300 ml of chloroform and NaOH-water solution (50 g–120 ml). The organic layer was washed three times with water. After it was dried over anhydrous sodium sulfate, the solvent was evaporated on a rotary evaporator to produce a pale yellow liquid. It was purified by silicagel column chromatography

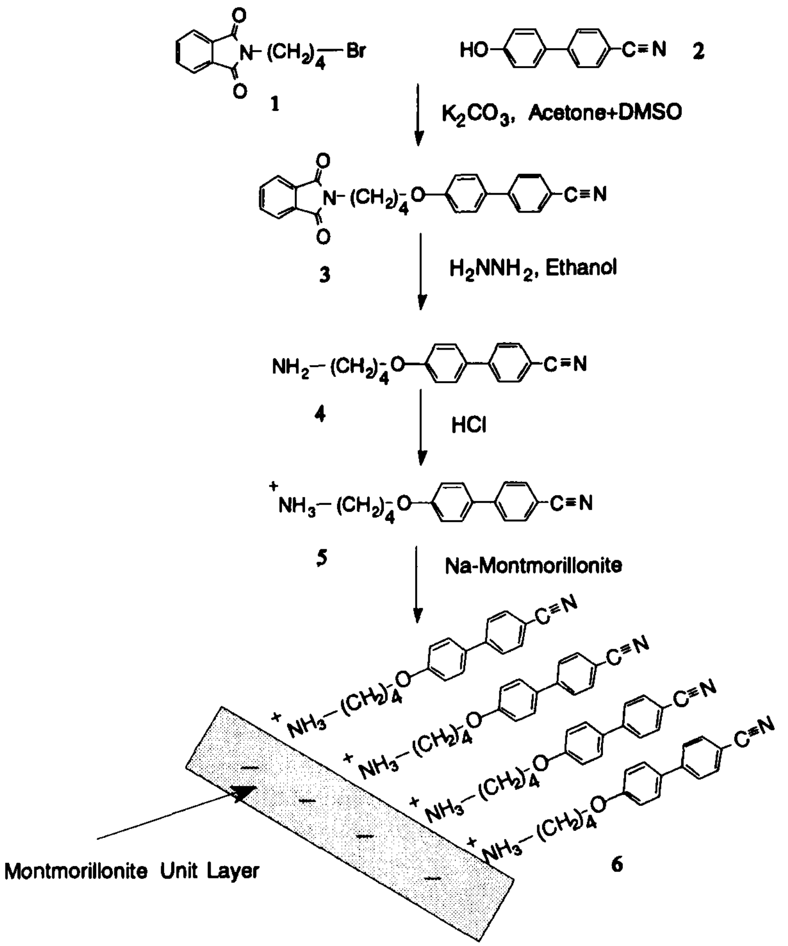

SCHEME 1 The preparation of motmorillonite intercalated with 4-(4′-cyanobiphenyl-4-oxy) butyl ammonium.

(solvent: ethanol: chloroform = 1:1) to yield a pale yellow solid (5.57 g) (yield, 60.0%). Melting point 102°C.

Intercalation

Sodium montmorillonite (6.31 g) was dispersed into water. 4-(4-Aminobutoxy)-4′-cyanobiphenyl (**4**) (2.20 g) and conc. hydrochloric acid (0.89 g) were dissolved into ethanol and water mixture (50 ml: 10 ml). It was poured into the montmorillonite-water solution under vigorous stirring to yield white precipitates. After 20 min, the precipitates were collected on a glass filter, washed with hot ethanol and two times with hot water, and freeze-dried to yield the montmorillonite intercalated with 4-(4′-cyanobiphenyl-4-oxy) butyl ammonium (**6**, CBAM, the content of the inorganic part, 75.0 wt%).

The preparation of LCCs based on 5CB and CBAM

The composites based on a liquid crystal and CBAM were prepared as follows. 5CB (1.0 g) was dissolved in DMSO (2.0 ml). CBAM (0.0256 g) was dispersed into DMSO and mixed with the 5CB solution. At this state, the unit layers of the montmorillonite dispersed homogeneously in DMSO. DMSO was evaporated in vacuo at 50°C to yield a white pasty composite (LCC-2, the content of the inorganic part, 1.9 wt%).

Two other composites with different contents of the inorganic parts (LCC-1 and LCC-3; the contents of the inorganic parts were 1.0 wt% and 2.9 wt%, respectively.) were prepared by the same method.

The preparation of LCC based on the montmorillonite intercalated with lauryl ammonium

The montmorillonite with lauryl ammonium (LAM) was prepared by the same procedure reported elsewhere[12].

5CB (1.0 g) was dissolved in DMAc (2.0 ml). LAM (0.0446 g) was dispersed into DMAc and mixed with the 5CB solution. DMAc was evaporated in vacuo at 50°C to yield a white pasty composite (LCC-LAM, the content of the inorganic part, 3.1 wt%).

Techniques

A Perkin-Elmer DSC-7 differential scanning calorimeter (DSC) was used to determine thermal transitions. Heating and cooling rates were 10°C/min in all cases.

An Olympus Model BHSP optical polarizing microscope (magnification, 500*x*) equipped with a Mettler FP-82HT hot stage and Mettler FP-90 central processor was used to observe thermal transitions and to analyze anisotropic textures.

A Rigaku Denki RAD-B X-Ray diffractometer was used to measure the interlayer distances of the intercalated montmorillonite and the montmorillonites in the LCCs.

A typical sample cell was indicated in Figure 1. The substrates of the cell are 1 mm thick glass plates coated with a thin transparent conductive In/SnO_2 (ITO) film to allow the application of electric fields across the LCC. The separation of the substrates is achieved by sandwiching the two plates with polymer beads spacer (diameter: 12 μm), thus defining the thickness of the LCC. The electro-optic effect and thermo-optic effect of the cells were measured by using the BHSP microscope equipped with a photomultiplier to monitor the optical change in the cell accompanying the application of electric fields across the samples (Fig. 1). These were reecorded on a chart recorder. In this case, the microscope was used without polarizers.

X-ray Diffraction Experiment

LCC-LAM was sandwiched between the polyester films (100 μm) coated with a transparent conductive electrode. The cell gap was 25 μm. A Rigaku Denki X-ray diffractometer RU-Z was used to detect the change in the alignment of the clay mineral in LCC-LAM cell by applying an electric field.

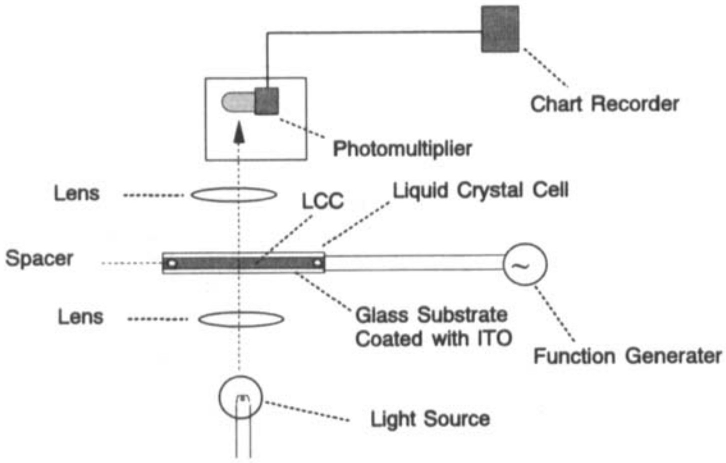

FIGURE 1 The schematic representation of the system set up for the optical measurements.

RESULTS AND DISCUSSION

5CB is a typical liquid crystal based on a cyanobiphenyl mesogenic unit (Scheme 2), which exhibits a nematic phase between 24°C and 34°C. It has a strong positive dielectric anisotropy and tends to align parallel to an applied electric field.

Montmorillonite is a layered clay mineral composed of aluminosilicate whose chemical composition is $(OH)_4Si(Al_{3.34}Mg_{0.66})O_{20}Na_{0.66}$. The dimension of the unit layer is 10 Å in thickness, about 1000 Å in width and in length. It has exchangeable cations between the layers, which are sodium cations. Therefore, the surface of the montmorillonite can be modified by exchanging sodium cations for organic onium ions such as alkyl ammonium cations. In this study, the montmorillonite exchanged with a mesogenic ammonium (**6**, CBAM) was used to enhance the miscibility between the montmorillonite and 5CB.

The Structure of LCC

The obtained LCCs are pasty liquids whose viscosity increases with increasing the content of the inorganic parts. The thermal properties of the obtained LCCs were measured by DSC and summarized in Table I. The nematic-isotropic transition temperatures of the LCCs on a second heating and first cooling are about 34°C and 29°C, respectively, and almost equal to those of pure 5CB. It means that the liquid crystallinity of 5CB in the LCCs is almost identical to that of pure 5CB. Figure 2

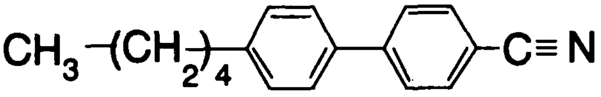

SCHEME 2 The chemical structure of 5CB.

TABLE I

The characterization of the obtained LCC and related compounds

Sample	CBAM content[a] (wt.%)	Interlayer distance[b] (Å)	Nematic (N)-isotropic (I) transition temp. (°C)	
LCC-1	1.0	19–21	Second heating First cooling	N 34 I I 29 N
LCC-2	1.9	25.2	Second heating First cooling	N 34 I I 29 N
LCC-3	2.9	25.2	Second heating First cooling	N 34 I I 29 N
K-15	–	–	Second heating First cooling	N 34 I I 30 N
CBAM	–	18.0	–	–

[a] Based on inorganic parts. [b] Measured by X-ray difractometer.

presents the typical polarized micrographs of LCC-2 in an isotropic state (a) and in a nematic state (b). In the isotropic state, only the particles of CBAM were observed as bright spots which were dispersed uniformly in the LCC. Their sizes are roughly estimated to be several micrometers or less. Therefore, they are aggregates of the unit layers of the montmorillonite.

The interlayer distance of the montmorillonite (the distance between the unit layers) were measured using a peak attributed to (001) plane of the montmorillonite by X ray diffractometer and summarized in Table I. The interlayer distance of the intercalated CBAM was 18.0 Å while those of CBAM in the LCCs were 19–25.2 Å. It means that some of 5CB was intercalated between the montmorillonite layers in the LCCs.

In the nematic state (Fig. 2b), the very fine texture of the LCC was observed. The texture is composed of very small domains of 5CB (multi-domain structure). Since pure 5CB does not exhibit such a texture, we concluded that the dispersed CBAM particles induced the multi-domain structure in the LCCs.

Electro-Optic and Thermo-Optic Effect

It was found that the LCC cells displayed interesting electro-optic and thermo-optic effects. Figure 3a and 3b shows a typical change in the transmittance of the LCC-2 cell by an electric field, shearing, and temperature change. Figure 4 presents the photographs of the LCC cell at various states. Initially, the cell scattered light strongly and the light transmittance was low (Fig. 3a and Fig. 4a). When an electric field was applied to the cell, it became transparent within 10–20 ms (on-state: 80 V–60 Hz, Figure 3a and Figure 4b). Interestingly, even after the electric field was switched off, although small decrease in the transparency was observed, the transparent state was maintained (Fig. 3a and Fig. 4c). We call this state memory state I. After 3 months, no change in the transparency of the memory state was observed. Figure 5 presents the dependence of the on-state and meemory state I transmittance of the LCC cells on an applied voltage. As the applied voltage was increased, the transmittance of the on-state increased gradually and saturated around 50–60 V. The content of CBAM in the LCCs also

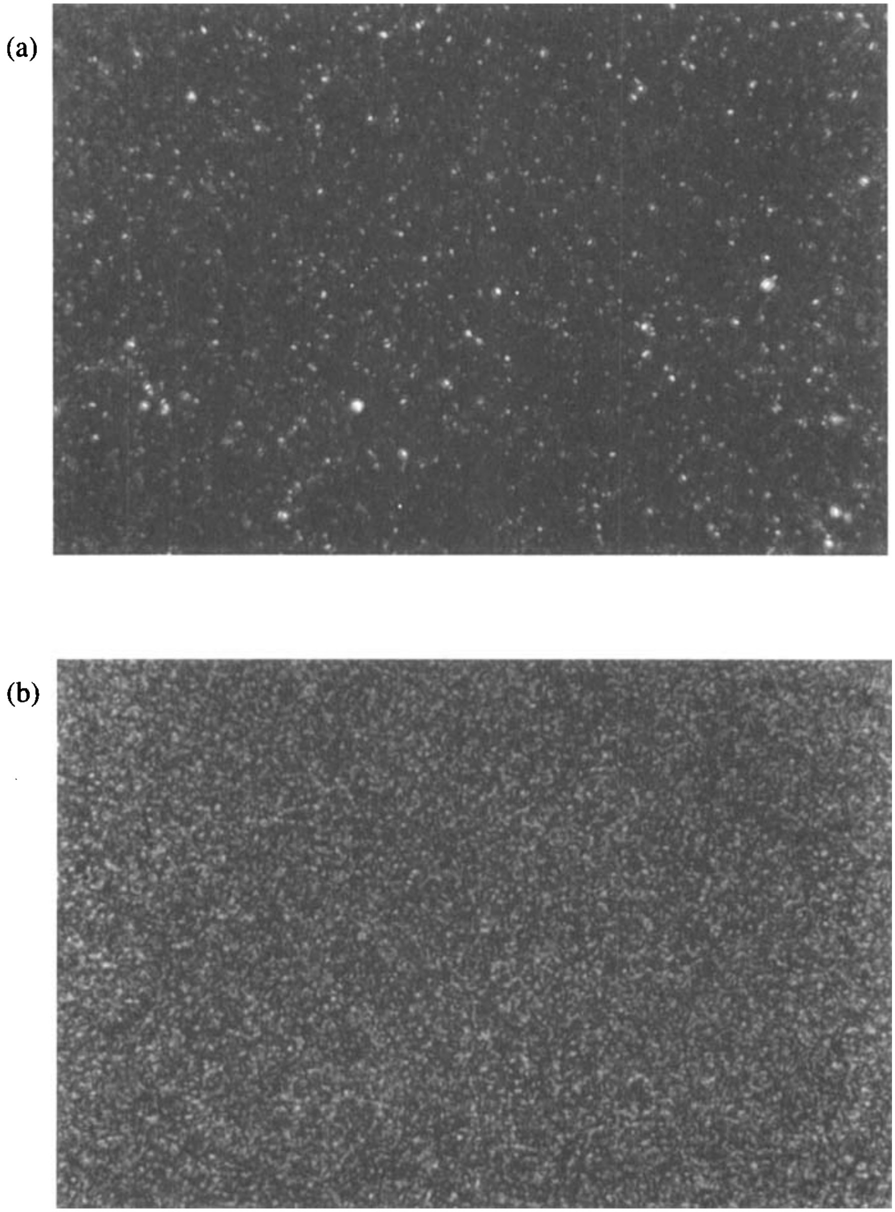

FIGURE 2 Optical polarized micrographs of LCC-2 (crossed nicol, the thickness of the sample is 12 μm): (a) isotropic state, (b) nematic state.

affects to the cell transmittance. As the content was increased, the cell transmittance decreased in all the states. The same trend as observed for the on-state transmittance was observed for the memory state I. In order to cancel the memory state to the initial state, a slight shearing should be given to the substrates of the cell (Fig. 3a).

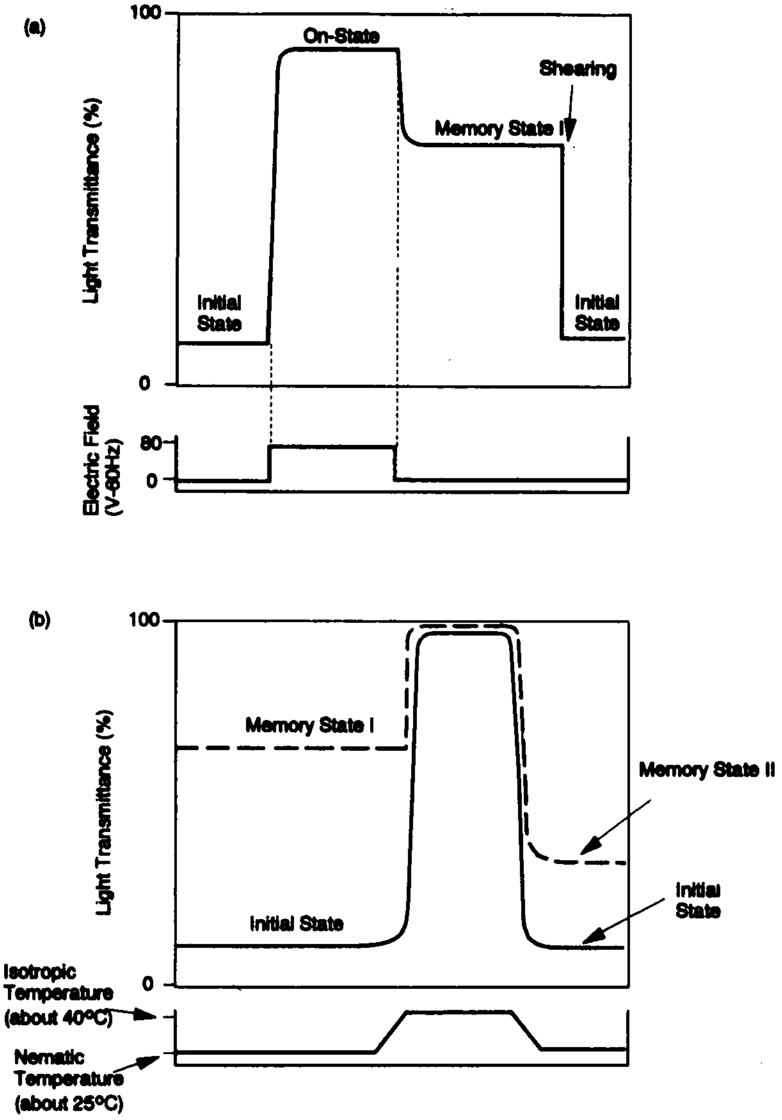

FIGURE 3 The typical change in the transmittance of LCC-2 cell(cell gap: 12 μm) by various external fields: (a) electric field and shearing at liquid crystalline temperature (about 25°C), (b) thermal change.

When the cell was warmed up above its isotropic temperature, it became transparent again (Fig. 3b and Fig. 4d). If the cell had not experienced an electric field, it returned to the initial state after cooling to the nematic temperature. However, when it had experienced an electric field, it went to a new state (memory state II) whose transparency stayed between the memory state I and the initial state (Fig. 3b). This unique thermo-optic effect could be used for laser-addressed storage displays in which information can be written on the LCC cell in memory

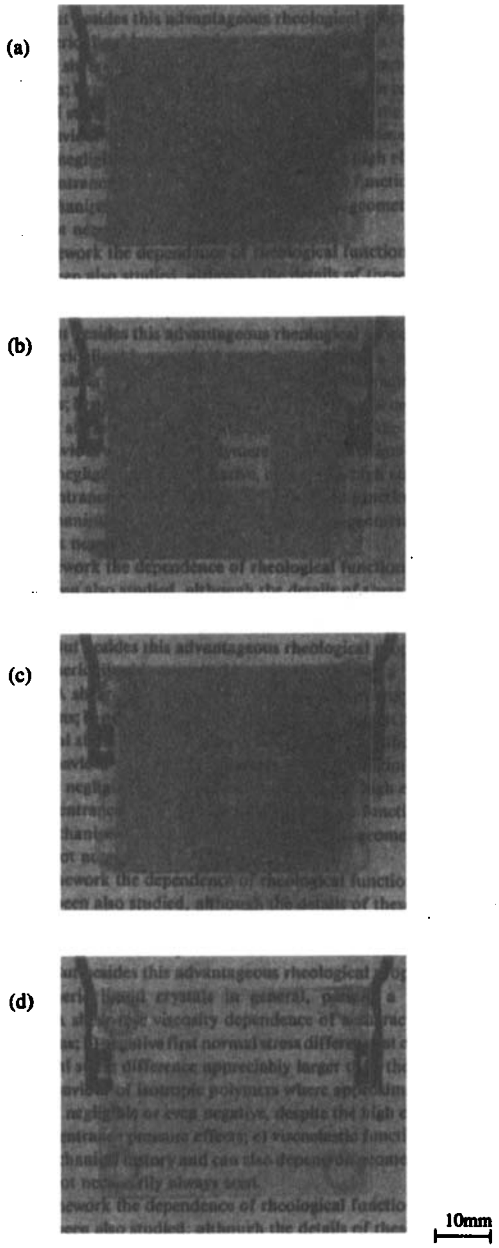

FIGURE 4 Photographs of the LCC-2 cell (cell gap: 12 μm) at various states: (a) initial light scattering state, (b) on state (100V – 60 Hz was applied only in a square region), (c) memory state I (the electric field is off), (d) isotropic state (about 40°C).

state I by using laser light beam and the stored information can be erased by an electric field.

The mechanisms of the electro-optic and thermo-optic effects of the LCC are proposed as follows. Figure 6 presents the schematic explanation of the electro-optic

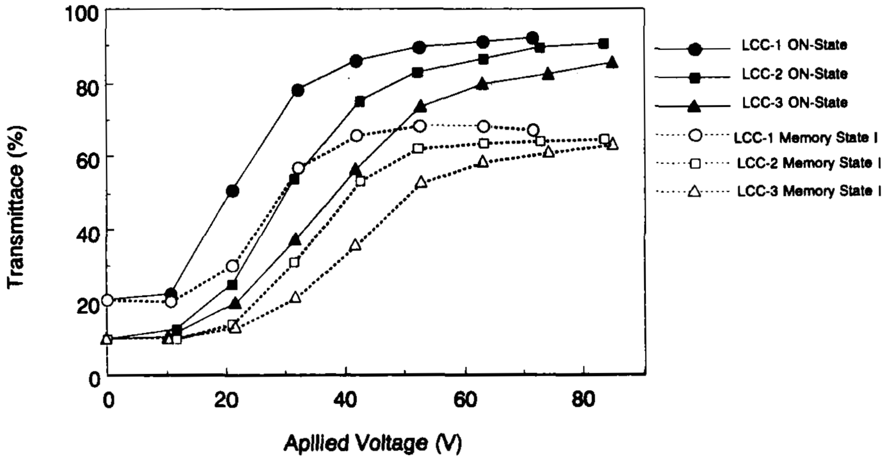

FIGURE 5 The dependence of applied voltage on the transmittance of the ON-State and the memory state I of the LCC cells.

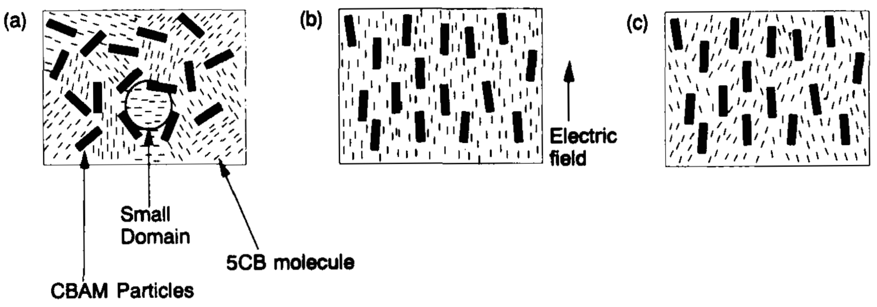

FIGURE 6 The schematic explanation of the mechanism for the electro-optic effect of the LCCs.

effect of the LCC cells. The light scattering effect of the LCC cell is attributed to its structure as follows. As discussed above, the LCC is composed of the small domains (Fig. 6a). The nematic director of each domain in the LCC is considered to orient randomly in space due to the presence of randomly oriented CBAM plates. Therefore, the fluctuation of refractive indexes is induced in the LCC and becomes the cause of light scattering. When an electric field is applied to the cell, not only 5CB but alsso CBAM plates align parallel to the electric field (Fig. 6b), and the cell gets transparent. Even after the electric field is switched off, the oriented plates maintain their orientation due to their bulkiness.

The alignemnt of the clay mineral plates in the LCC was proved by X-ray diffraction experiment as follows. In this experiment, the LCC-LAM based on LAM and 5CB (Clay content, 3.1 wt%) was used. Since it exhibited a sharper diffraction peak attributed to the (001) plane of the montmorillonite compared to those of the LCCs based on CBAM, it was much easier to detect the change in their alignments. The sample also exhibited the similar electro-optic and thermo-optic effects as explained above although the stability of the dispersed clay particles under an electric field was not as good as that of the LCC based on CBAM (In the case of the LCC-LAM, the particles tend to aggregate each other under an electric field.). Figure 7 indicates the transmission X-ray diffraction pattern of the LCC-LAM cell. Before the addition of an electric field, the (001) peak was small, while, after the application of an electric field, it apparently became stronger than before. This is due to the fact that the montmorillonite plates aligned parallel to the applied electric field (Fig. 8).

5CB also maintains its homeotropic alignment, thus producing the memory state I (Fig. 6c). The transparency at the memory state I is not as high as that at the on-state. This may be attributed to the imperfect homeotropic alignment of 5CB due to the absence of the electric field. When the cell is warmed up to the isotropic temperature, the multidomain structure of 5CB disappears and the only light scattering factor remained becomes the mismatching of refractive indexes between the isotropic 5CB and CBAM. Since the amount of the clay is mere few weight percents, the light

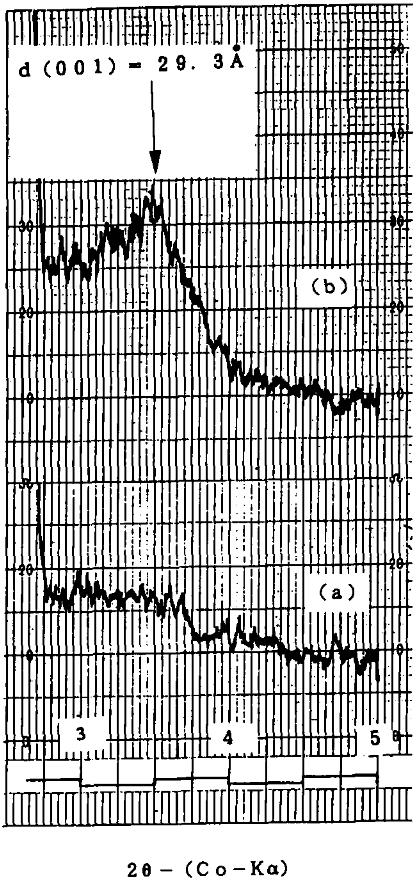

FIGURE 7 Transmission X-ray diffraction patterns of the LCC-LAM cell: (a) before the application of an electric field (initial state), (b) after the application of the electric field (100 V – 60 Hz, memory state I).

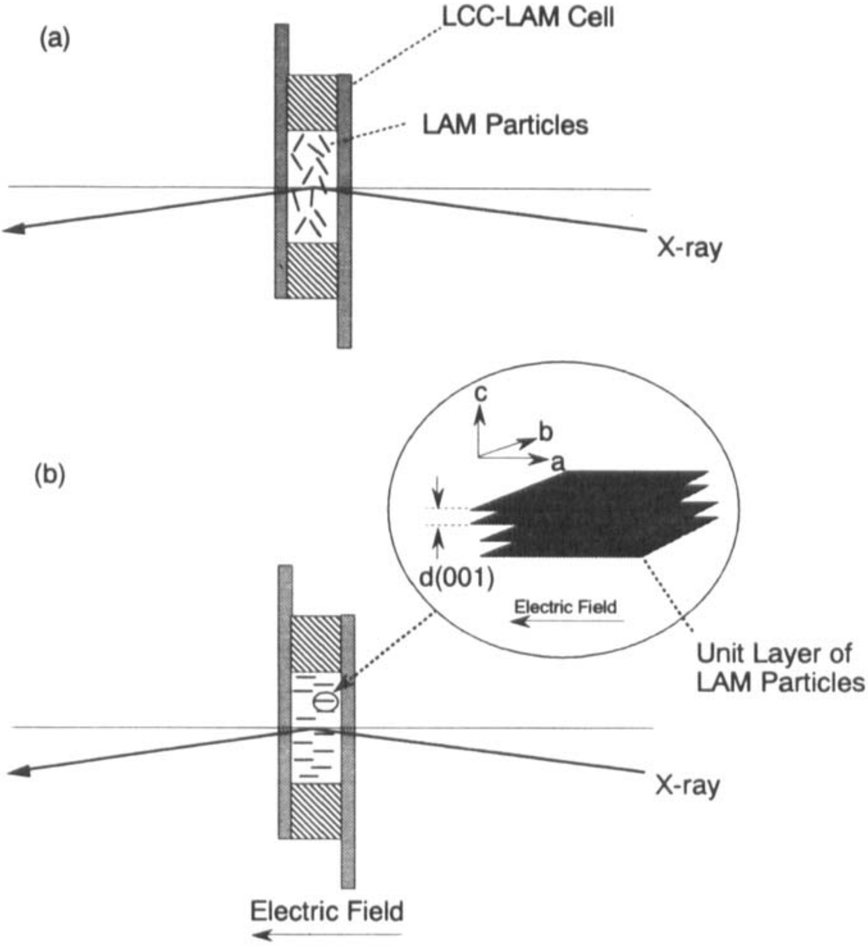

FIGURE 8 The change in the direction of the clay particles with respect to that of X-ray beam by an electric field: (a) before the application of an electric field (initial state), (b) after the application of the electric field (memory state I).

scattering effect is negligible. Therefore, the cell gets almost transparent regardless of the state of the LCC. The two states appear after cooling from the isotropic state depending on whether the state before heating is the initial state or the memory state I (Fig. 3b). This may be due to the difference in the alignments of CBAM plates in the memory state I and the initial state since the alignment of CBAM at the memory state does not change so much by heating. However, the detailed explanations has not been obvious yet.

CONCLUSIONS

By mixing the liquid crystal and organophilic clay mineral, we could have created the novel liquid crystalline composities in which the plates of the clay mineral were homogeneously dispersed in micrometer level. The composites exhibited an unique light scattering effect with memory effect which could be controlled by electric field, temperature change, and shearing. This new material would be a potential candidate for advanced applications such as an erasable optical storage device, thermo-optical sensor device, and so on. Also, the results shown in this paper would open a new opportunity to synthesize a variety of liquid crystalline composites and to extend the functions of liquid crystals.

References

1. G. H. Heilmeier and J. E. Goldmacher, *Appl. Phys. Lett.* **13**, 132 (1968).
2. W. Haas, J. Adams and G. Dir, *Chem. Phys. Lett.* **14**, 95 (1972).
3. G. H. Heilmeier and J. E. Goldmacher, *Prox. IEEE.* **57**, 34 (1969).
4. R. A. Soref, *J. Appl. Phys.* **41**, 3022 (1970).
5. W. Haas, J. Adams and J. B. Flannery, *Phys. Rev. Lett.* **24**, 577 (1970).
6. J. P. Hulin, *Appl. Phys. Lett.* **21**, 10 (1972).
7. S. Morimoto, A. Miyamoto, H. Kikuchi and T. Kajiyama, *Rept. Progr. Polym. Phys. Jpn.* **31**, 191 (1988).
8. T. Kajiyama, H. Kikuchi, A. Miyamoto, S. Moritomi and J. C. Hwang, *Chem. Lett.* **1989**, 817 (1989).
9. T. Kajiyama, H. Kikuchi, A. Miyamoto, S. Moritomi and J. C. Hwang, *Mat. Res. Soc. Symp. Proc.* **171**, 305 (1990).
10. R. Yamaguchi and S. Sato, *Liq. Cryst.* **14**, 4, 929 (1993).
11. R. Yamaguchi, H. Ookawara, M. Ishigame and S. Sato, *Journal of the SID* **1**, 347 (1993).
12. K. Yano, A. Usuki, A. Okada and O. Kamigaito, *J. Polym. Sci. Poly. Chem.* **31**, 2493 (1993).